

Living Diatom Microalgae for Desiccation-Resistant Electrodes in Biophotovoltaic Devices

Cesar Vicente-Garcia, Danilo Vona, Francesco Milano, Gabriella Buscemi, Matteo Grattieri, Roberta Ragni,* and Gianluca M. Farinola*



Cite This: *ACS Sustainable Chem. Eng.* 2024, 12, 11120–11129



Read Online

ACCESS |

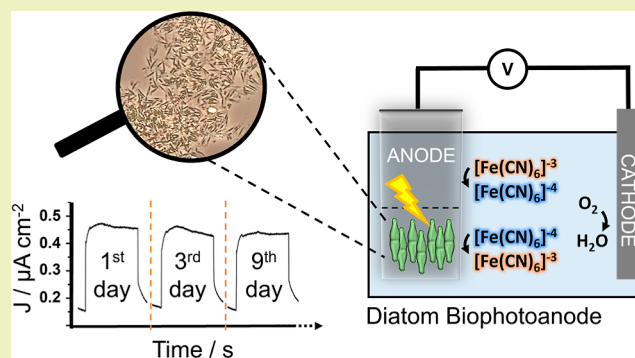
Metrics & More

Article Recommendations

Supporting Information

ABSTRACT: Strategies of renewable energy production from photosynthetic microorganisms are gaining great scientific interest as ecosustainable alternatives to fossil fuel depletion. Green microalgae have been thoroughly investigated as living components to convert solar energy into photocurrent in biophotovoltaic (BPV) cells. Conversely, the suitability of diatoms in BPV cells has been almost completely unexplored so far, despite being the most abundant class of photosynthetic microorganisms in phytoplankton and of their good adaptability and resistance to harsh environmental conditions, including dehydration, high salinity, nutrient starvation, temperature, or pH changes. Here, we demonstrate the suitability of a series of diatom species (*Phaeodactylum tricornutum*, *Thalassiosira weissflogii*, *Fistulifera pelliculosa*, and *Cylindrotheca closterium*), to act as biophotoconverters, coating the surface of indium tin oxide photoanodes in a model BPV cell. Effects of light intensity, cell density, total chlorophyll content, and concentration of the electrochemical mediator on photocurrent generation efficiency were investigated. Noteworthy, biophotoanodes coated with *T. weissflogii* diatoms are still photoactive after 15 days of dehydration and four rewetting cycles, contrary to analogue electrodes coated with the model green microalga *Dunaliella tertiolecta*. These results provide the first evidence that diatoms are suitable photosynthetic microorganisms for building highly desiccation-resistant biophotoanodes for durable BPV devices.

KEYWORDS: biophotoelectrochemical cell, biophotoanodes, photocurrent, diatom microalgae, dryness resistance



INTRODUCTION

The worldwide energy demand has been continuously increasing over the last decades, with the trend expected to rise in the next future.¹ Despite the current huge global efforts, technologies for sustainable energy production from renewable sources are still at an early stage, and green-energy supply is far from the levels achieved by nonrenewable sources.² Solar panels, wind turbines, or geothermal stations are beneficial alternatives to fossil-fuel-based energy platforms, reducing the exhaust gas release responsible for climate change. Nevertheless, low recyclability and lifespan of materials used for such technologies currently limit their integration into a circular economy approach.³ In the last two decades, microbial fuel cells (MFCs) have emerged as alternative biobased platforms for green energy or fuel production. MFCs are electrochemical systems powered by redox reactions catalyzed by living organisms that interact with an abiotic interface.⁴ Although artificial materials are still needed to fabricate the electrical and conductive elements of these devices, the photochemical reactions leading to solar energy conversion are carried out by living microorganisms, which represent intrinsically renewable

biomaterials optimized by Nature, and available at large scale and low cost.

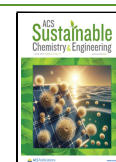
MFCs based on photosynthetic organisms are also known as biophotoelectrochemical cells (BPECs), and they avail of whole photosynthetic microorganisms, intact parts such as organelles, or just isolated photosynthetic proteins as bioactive components.⁵ BPECs based on oxygenic photosynthetic microorganisms, defined as biophotovoltaic (BPV) cells, feature the major advantage versus other MFCs of electrical power generation through water photolysis in the absence of exogenous supply of organic nutrients and with concomitant removal of CO₂ from the external environment. The use of intact photosynthetic microorganisms has several advantages, such as enhanced stability or self-replication, but also the drawback of difficult interaction between the biological catalyst

Received: January 31, 2024

Revised: May 16, 2024

Accepted: May 17, 2024

Published: May 30, 2024



and the abiotic electrode interfaces. Hence, BPVs' sustainability and efficiency are strictly dependent on the choice of appropriate microorganisms, and in particular on their electrogenic capacity, affinity with the electrode material, and resilience and compatibility with the device working conditions.⁶ Representative examples of organisms used in BPVs include cyanobacteria,⁷ eukaryotic microalgae,⁸ and more recently even macroalgae.⁹

BPVs based on diatom microalgae are currently under-represented, with very rare investigations reported so far in the literature,^{10,11} despite their interesting characteristics. In fact, diatoms are unicellular photosynthetic microorganisms that represent the most abundant species of phytoplankton. They live in suspension (planktonic diatoms) or adhering to substrates (benthonic diatoms), both in freshwater and marine habitats.¹² With respect to green and red microalgae, diatoms better adapt and survive to environmental changes of salinity,¹³ pH, and temperature,¹⁴ due in part to the presence of nanostructured biosilica shells (frustules) that protect cells protoplasm from mechanical, biological, and radiative stress factors, while allowing the free exchange of nutrients and other elements.¹⁵ Being mainly autotrophic, they easily grow even in low-nutrient environments.¹⁴ The broad availability of diatoms in all marine ecosystems also enables them to be cultured at a large scale, thus envisaging their application as bio factories of high added-value products such as pigments, oils, biofuel,¹⁶ and nanostructured biosilica-based materials for medicine,¹⁷ photonics,¹⁸ optoelectronics,¹⁹ and environmental bioremediation.²⁰ Diatoms also bear profitable features for application in BPEC solar energy conversion technologies because benthonic microalgae can generate biofilms adhering to a variety of materials,²¹ such as electrodes' surfaces, thus allowing their spontaneous colonization. Their biofilms are also rich in bioactive molecules and proteins,^{22,23} with unexplored electron-transfer potential. In principle, chemical modification of diatoms with tailored materials with conductive properties may be a powerful tool to face one of the most important challenges in BPV design i.e., favoring electrical communication between the biotic (microalgae) and abiotic (electrode) elements.²⁴ Moreover, due to their ability to withstand extreme conditions like water starvation and desiccation,^{25,26} diatoms are promising candidates for BPVs. In fact, whether the bioanode preparation includes a desiccation step, they would not need protection into hydrogels or other encapsulating materials that are conversely essential for dryness suffering species.²⁷ Moreover, persistent light irradiation or aqueous medium evaporation are common issues expected for BPVs working under practical uncontrollable conditions, making crucial the choice of very resistant photosynthetic microorganisms.²⁸ For example, the desiccation-resistance of microalgae could enable easy transport and dry state storage. In this way, BPVs could be activated by adding an electrolyte, and they could be switched-on/off providing or withholding moisture.

Diatoms are expected to have significant electrogenic capacity,¹⁰ since their membrane oxidoreductase enzymes are highly expressed.²⁹ These proteins have important roles in signaling, growth, and even interaction of microalgae with other microorganisms. Membrane oxidoreductases with ferriredoxase (FR) activity play an important role in electrogenic capacity, being related to the photosynthetic electron transport.³⁰ Moreover, NADPH oxidases are supposed to produce superoxide species outside the cell via

plasma membrane electron transport.³¹ Literature also reports that the enhancement of membrane NADPH oxidase activity in *Phaeodactylum tricornutum* diatoms leads to increased photocurrent production in BPVs working with potassium ferricyanide (K-ferricyanide) as an exogenous soluble mediator.¹⁰ On this ground, the high electrogenic capacity and resistance of diatoms to stress conditions are significant features motivating the need of an in-depth investigation of the suitability of these microorganisms as bioactive components in BPVs, these aspects being not yet systematically studied with respect to other microalgae candidates.

Herein, we provide a systematic investigation of the performance of diatom-based BPV cells with a three-electrode configuration, where an indium tin oxide (ITO) working electrode (WE) is coated with a series of diatom species, namely *P. tricornutum*, *Thalassiosira weissflogii*, *Fistulifera pelliculosa*, and *Cylindrotheca closterium*. The effects of the electrode coating procedure, deposited cell density, electrochemical mediator concentration, light intensity, and electrochemical potential on the biophotoanode performance have been evaluated to set the best experimental working conditions of the BPV.

To the best of our knowledge, this study provides the first evidence that the biophotoanodes prepared by the *T. weissflogii* diatom, selected as the best performing species, keep their photoactivity in BPV cells, resisting a series of desiccation/rewetting cycles and repeated photocurrent extraction much better than biophotoanodes from the model green microalga *Dunaliella tertiolecta*.

EXPERIMENTAL SECTION

Materials and Reagents. All chemicals were used as received without further purification. Ultrapure grade acetone, ethanol, K_2HPO_4 , KH_2PO_4 , $K_3[Fe(CN)_6]$ (K-ferricyanide), $K_4[Fe(CN)_6]$ (K-ferrocyanide), sodium bicarbonate, *N,N*-dimethylformamide (DMF), F/2 Guillard concentrate 50X, Hellmanex III solution, fluorescein diacetate (FDA), and ITO-coated glass slides were purchased from Sigma-Aldrich (Germany). All aqueous solutions were prepared using deionized water obtained by a Milli-Q Gradient A-10 system (Millipore, 18.2 M Ω cm, organic carbon content $\leq 4 \mu g L^{-1}$). ITO glass slides of $1.8 \times 0.8 \text{ cm}^2$ area, 0.7 mm thickness, $\sim 60 \Omega \text{ sq}^{-1}$ surface resistivity, and a transmittance $>85\%$ were used for the preparation of bioelectrodes.

Microalgae Growth. *P. tricornutum* (CCAP strain 1055/1, Pht), *T. weissflogii* (CCAP strain 1085/18, Tw, also known as *C. weissflogii*), *F. pelliculosa* (CCAP strain 1050/9, Fp, formerly known as *Navicula pelliculosa*), *C. closterium* (Nantes Cultures Collection, Cc), and *D. tertiolecta* (CCAP strain 19/24, Dt) were grown inside a vertical incubator with controlled temperature and relative humidity ($18 \pm 2^\circ \text{C}$, 65%) under a photosynthetically active radiation of $20\text{--}40 \mu \text{mol} \cdot \text{m}^{-2} \cdot \text{s}^{-1}$ measured by a MSC15 Spectral Light Meter (Gigahertz Optik, Germany), provided by two white fluorescent tubes (6500 K, 30 W) on a 16/8 h light/dark cycle. Cultures were grown in F/2 Guillard prepared with sterile natural seawater (28 practical salinity units), buffered with 1 mM NaHCO_3 at pH = 7.8, in polystyrene flasks (250 mL) without stirring. Half of the culture volume was substituted with fresh medium every 2 weeks, and splitting was performed once a month. Cells used for bioelectrochemical measurements were collected between the late exponential and early stationary growth phases.

Preparation of Biophotoanodes. ITO-coated glass slides were used to prepare the microalgae-based bioanodes. Cell density was determined by using a Bürker cell counting chamber. Cells were recovered at 360g for 12 min at room temperature (RT). For the preparation of each bioanode, the microalgae pellet was suspended in 20 μL of 90 mM phosphate buffer (PB) pH = 7.8, spotted onto ITO

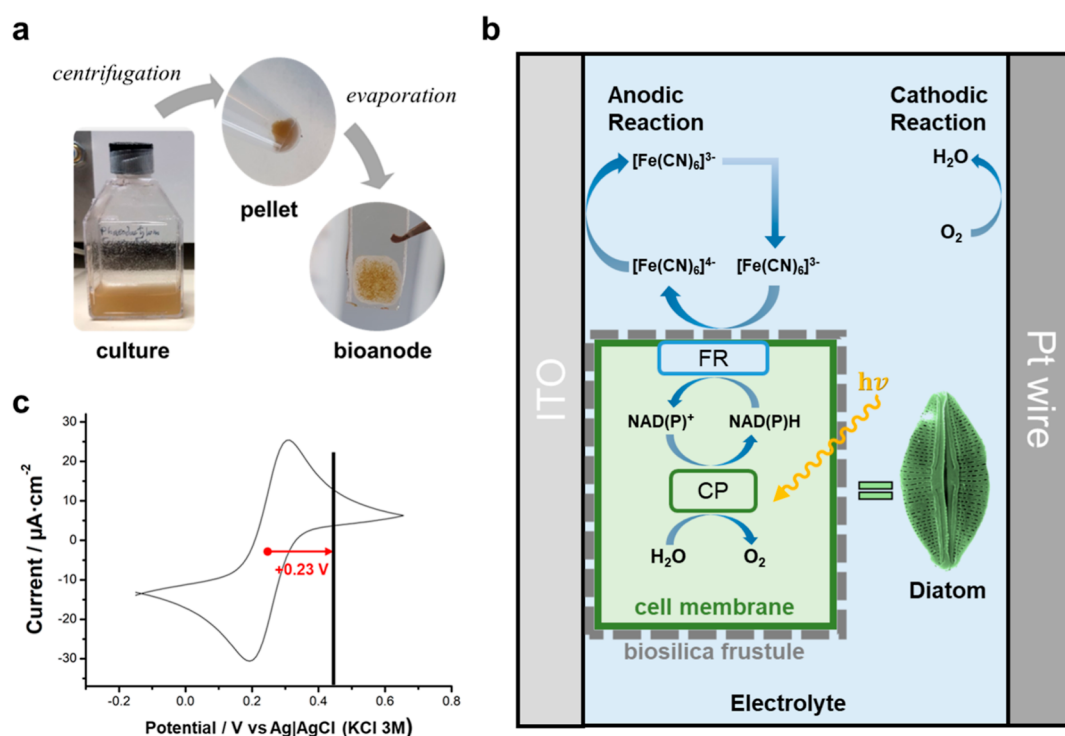


Figure 1. (a) Preparation of the air-dried diatom bioanode from a fresh culture of diatoms. The white matrix around the diatom spot corresponds to residual salts from the culture medium. (b) Scheme of the photoelectrochemical cell representing the microalgae onto ITO WE, the frustule, the cell membrane, the chloroplast (CP) inside the microalgae, the membrane ferredoxin (FR), the K-ferro/ferricyanide couple in PB solution, and the platinum wire CE. The reference electrode has not been depicted for simplicity, and the different phases are not in scale. (c) Cyclic voltammogram performed at a 20 mV·s⁻¹ scan rate with the ITO electrode coated with 10⁶ cells and immersed in a solution containing 0.5 mM K-ferricyanide; the red arrow shows an overpotential of +0.23 V with respect to E_{1/2} of the ferro/ferricyanide couple applied in the CA experiments.

slide coating an area of 0.8 cm² (0.8 × 1.0 cm²) prior to air-dry (Figure 1a). This methodology allows us to obtain artificial films of diatoms onto an ITO slide containing a known number of cells (10⁶ cells per slide, unless stated otherwise). ITO slides were reused after a thorough washing routine (sonication in 5% Hellmanex III solution, followed by sonication in deionized water, rinsing with acetone, and finally drying under a fume hood). A Cary 5000 UV–vis–NIR spectrophotometer (Agilent Technologies Inc. USA) was used to record the absorbance spectra of the dry biophotoanodes for the calculation of the internal quantum efficiency (IQE).

Electrochemical Setup. All electrochemical measurements were performed by an Autolab potentiostat PGSTAT 10, using a 1 mL polystyrene open photoelectrochemical cell (1.0 × 1.0 × 1.0 cm³) with a three-electrode configuration, and PB as the electrolyte (Figure 1b). The transparent ITO slide coated with the microalgal film was used as the WE with a submerged area of 0.8 cm² to perform the anodic reaction. A platinum (Pt) wire with 0.314 cm² estimated submerged area (*r* = 0.05 cm; *h* = 1.00 cm) and Ag|AgCl (KCl 3 M) were used as the counter (CE) and reference (RE) electrodes, respectively. K-ferricyanide was used as the soluble electrochemical mediator at a 0.5 mM concentration (unless stated differently). To ensure a sufficient overpotential to drive the oxidation reaction of the redox mediator, chronoamperometry (CA) measurements were performed at a potential 0.23 V higher than the half-wave potential (E_{1/2}) of the K-ferro/ferricyanide couple. E_{1/2} was evaluated by cyclic voltammetry (20 mV·s⁻¹ scan rate) immediately prior to every CA experiment to avoid undesired potential variations that may occur upon any change of bioanode (Figure 1c). The system was illuminated by a white LED bulb (3000 K, from 425 to 725 nm, with maximum emission peaks at 455 and 600 nm), with 54 mW·cm⁻² light intensity at 5.5 cm working distance (unless stated differently), measured by a MSC15 Spectral Light Meter (Gigahertz Optik, Germany). The white LED was purposefully chosen because its emission appropriately fits with the absorption of the microalgae

photosynthetic pigments (Figure S1). Light/dark cycles of 300 s were applied during the CA measurements. The system was unstirred, at 20–25 °C, and covered by a black velvet fabric to guarantee complete darkness. All CA experiments were performed in triplicate under the following set conditions, unless otherwise stated: 1 mL PB, 0.5 mM K-ferricyanide, *P* = E_{1/2} (K-ferro/ferricyanide) + 0.23 V, 54 mW·cm⁻² white light intensity, 4 light cycles of 300 s, 45 min total time under applied potential, RT, and unstirred.

Cell Viability Studies. Morphology and viability of the cells in liquid cultures, as well as of the cells coating the bioanodes, were checked by means of epifluorescence microscopy with an Axiomat Zeiss microscope (Oberkochen, Germany) using a TRITC filter set, through evaluation of chlorophyll fluorescence of chloroplasts (λ_{ex} = 568 nm, λ_{em} > 600 nm). To further evaluate the viability of microalgae before and after CA measurements, the FDA assay was used. FDA is a nonpolar, nonfluorescent molecule that can passively diffuse through cellular membranes and accumulate inside cells. Only when in contact with living cells, it can be hydrolyzed by esterases to a green fluorescent derivative exclusively staining the living cells.³² Cells were centrifuged at 360g for 12 min at RT and the cell pellet was suspended in 1 mL of PBS and a FDA acetone solution (12 μL, 5 mM) was added. The mixture was incubated in the dark for 1.5 h and transferred to a flat-bottom 96-well transparent plate. Fluorescence intensity at 511 nm was recorded (λ_{ex} = 488 nm) by a Spark Multimode Microplate Reader (Tecan, Switzerland) and it was used to evaluate and compare the viability of each sample (normalized to 10⁶ cells) after subtracting the background signal from the sole buffer and normalizing the highest sample to 100%.³³

Total Chlorophyll Quantification. For total chlorophyll quantification, fresh samples from each species were used. Cells were stirred in DMF (2 mL of DMF/10⁶ cells) at 4 °C in the dark, for 24 h. Cells were then centrifuged for 12 min at 4000g. Absorption spectra of the supernatant were recorded in the 250–900 nm range using a Cary 5000 UV–vis–NIR spectrophotometer (Agilent

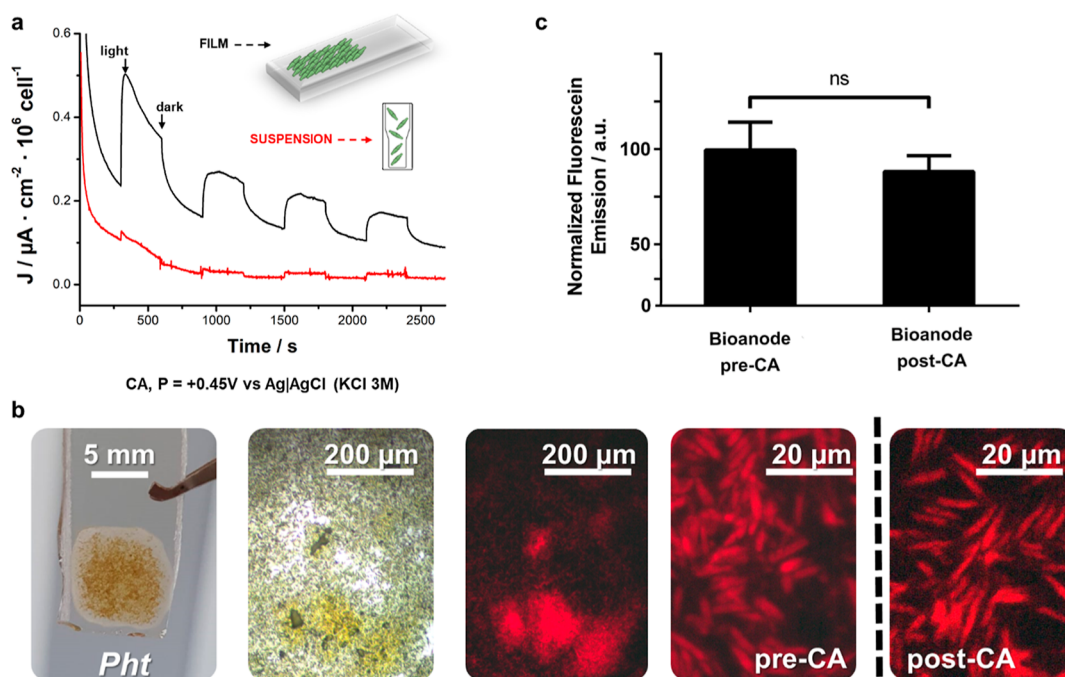


Figure 2. (a) Photocurrent signals from 10^6 Pht cells in suspension (red) and 10^6 Pht cells coated ITO bioanode (black). (b) Images of a Pht-coated ITO bioanode, from left to right: macroscopic view, bright field microscopy image at 20X, fluorescence microscopy images ($\lambda_{\text{ex}} = 568 \text{ nm}$, $\lambda_{\text{em}} > 600 \text{ nm}$) at 20X, at 100X before CA, and at 100X after CA. (c) Mean fluorescein emission ($\lambda_{\text{ex}} = 488 \text{ nm}$, $\lambda_{\text{em}} = 511 \text{ nm}$) in the FDA viability assay of Pht cells performed before and after CA.

Technologies Inc., USA). The total chlorophyll content was calculated as follows: total chlorophyll ($\text{mg} \cdot \text{L}^{-1}$) = $7.74 \times A_{664} + 23.39 \times A_{630}$.¹⁰

Statistical Analysis. Statistical tests were performed using GraphPad Prism (v.6.0.1). The paired two-tailed Student *t* test was used for pairwise comparisons, while two-way ANOVA followed by Sidak multiple comparisons test were performed for multiple comparisons. Statistical significance was assessed using *p* < 0.05. *P* values lower than 0.01 and 0.001 are marked with two and three asterisks, respectively.

RESULTS AND DISCUSSION

The BPEC was assembled in accordance with the well-known three-electrode configuration,³⁴ selecting robust and standard materials that are commonly used in the literature for photoelectrochemical systems. Likewise, for the setup optimization, *P. tricornutum* (Pht) was selected as the model diatom species to be deposited on the bioanode due to its well-known adaptability and resilience under harsh conditions.¹⁵ Indeed, Pht shows several properties desirable for BPV applications, such as the ability to form adhesive biofilms that can colonize the surface of an electrode, as well as the capacity to thrive even under low-nutrient conditions, ensuring long-lasting cultures.³⁵ Setup parameters optimized by using the Pht-coated bioanodes were then applied to all experiments carried out with different microalgal species.

Implementation of the Photoelectrochemical Setup and Bioanode Fabrication. The photoelectrochemical system was designed to enable photocurrent extraction from living microalgae with fair efficiency and reproducibility. ITO-covered glass was chosen as the anode due to its good interaction and compatibility with diatom microalgae.³⁶ Cyclic voltammetry of the K-ferro/ferricyanide couple was carried out to select the appropriate potential to be applied to the WE in the presence of living microalgae. Since the photosynthetic

activity of microalgae is expected to reduce K-ferricyanide, the applied external potential must be selected to reoxidize ferrocyanide and regenerate the mediator at the surface of the anode (ITO). For this reason, the applied potential for CA was set at +0.23 V vs $E_{1/2}$ of the mediator redox couple.

Adsorption of photosynthetic microorganisms onto the WE surface is a profitable strategy to favor the interaction between electrode, mediators, and living cells involved in the anodic reaction.^{32,37} Indeed, this strategy allows confinement of the processes leading to photocurrent next to the bioanode. For this aim, the model Pht diatom cells were concentrated into a small volume, drop-casted onto the ITO surface and air-dried at RT. The resulting bioanode coated with 10^6 cells yielded photocurrents with a good signal-to-noise ratio and good repeatability after the first cycle ($\sim 100 \text{ nA}/\text{cm}^2$ at the fourth illumination cycle) (Figure 2a, black trace). Conversely, the use of Pht cells in suspension produced much lower photocurrents with worse signal-to-noise ratio (Figure 2a, red trace). Time stability of the microalgal film was confirmed by observing that fewer than 1% of Pht cells detach from the bioanode after one CA measurement lasting 45 min (Figure S2).

The partial dehydration process used for the bioanode preparation is expected to stress cells. Bright field and fluorescence microscopy images of the bioanode were acquired to evaluate cell viability before and after CA measurements. The strong red fluorescence, upon green light excitation of chlorophylls, confirmed chloroplast integrity (Figure 2b),³⁸ indicating that Pht diatoms are still intact after being subjected to an overall 45 min experiment of photocurrent extraction in the presence of the K-ferricyanide mediator, including four photoexcitation cycles (5 min light/5 min dark each). This outcome further confirms the ability of Pht diatoms to interact with K-ferricyanide as previously reported in the literature.¹⁰

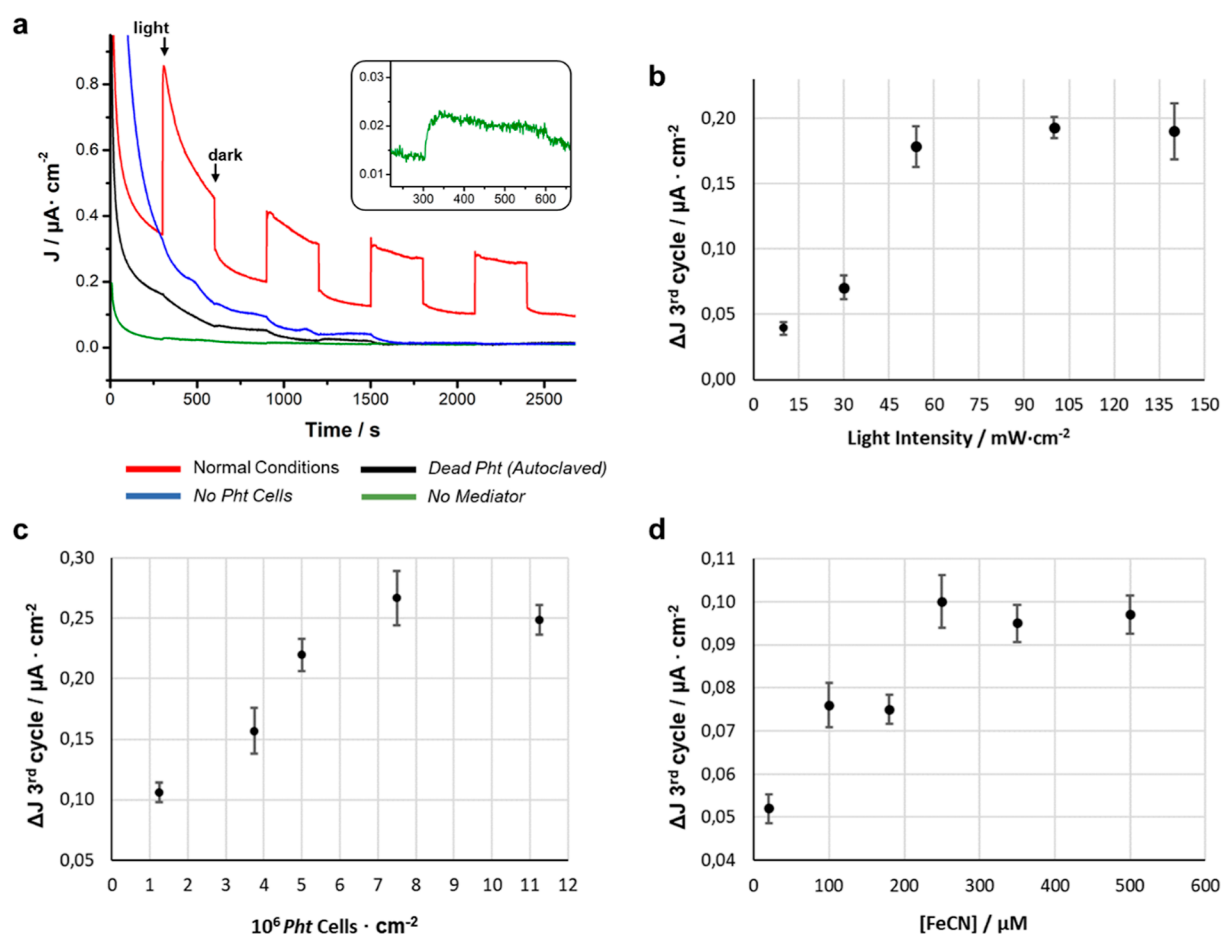


Figure 3. (a) Photocurrent measurements carried out: under the standard conditions reported in the Experimental Section (red line); using bare ITO as the WE (blue line); in the absence of K-ferricyanide mediator (green line); and using Pht cells after an autoclave cycle (121 °C, 15 psi, 20 min). Inset: detail of the photocurrent signal from Pht in the absence of K-ferricyanide. Photocurrent values on the third cycle of illumination at increasing (b) light intensity (10, 30, 54, 100, and 140 $\text{mW} \cdot \text{cm}^{-2}$), (c) cell density of Pht cells onto ITO surface, and (d) concentration of K-ferricyanide mediator.

This result is also supported by the FDA viability test, which shows no significant difference in the viability of Pht cells before and after the CA measurement (Figure 2c).

Photocurrent Dependence on Living Cell Photosynthetic Activity and Setup Optimization. To demonstrate the key roles of the viable photosynthetic cells deposited onto ITO and of the K-ferricyanide mediator, a series of control experiments were performed. Upon using a bare ITO electrode instead of the Pht-coated analogue, no photocurrent was observed (Figure 3a, blue line), thus excluding any contribution from the sole redox mediator. The same result was obtained when the bioanode was prepared by using Pht cells thermally inactivated at 120 °C (Figure 3a, black line). Moreover, in the absence of the K-ferricyanide mediator, only a small photocurrent signal was observed (Figure 3a, green line, inset). This indicates that the soluble mediator is the main species responsible for the extracellular electron transfer between diatoms and the electrode under the conditions studied. However, the presence of a non-negligible photoresponse from the bioanode without the exogenous redox mediator, despite being of low intensity, suggests the presence of redox active metabolites suitable as endogenous mediators, enabling electron transfer from cells to the electrode (Figure 3a, inset). Redox active biological molecules that facilitate electron transfer have been already described for photo-

synthetic microorganisms, like endogenous quinones or NADPH.²⁴ A direct electron transfer from diatom cells to ITO seems unlikely since no natural conductive structures have been previously described for diatoms. However, the presence of endogenous mediators cannot be completely ruled out, since the biosilica is enfolded in a complex network of biomolecules, including polyphenols and NADPH, that could potentially possess some electron-transfer capabilities.^{22,39} Moreover, electron transfer can occur via extracellular material secreted by biofilm-forming photosynthetic microorganisms like cyanobacteria,³⁷ a property that could be shared by a benthonic diatom such as Pht. Even though the bioanode used constitutes an artificial film and is not a natural biofilm, extracellular material is likely entrapped in the Pht pellet that serves as a starting material for the bioanode fabrication. Therefore, despite being of low intensity, the photocurrent signal reported in the inset of Figure 3a is interesting since it suggests the possibility to avoid the use of an external mediator if biotechnological methods are employed to boost production of endogenous mediators by cells.

The photocurrent output of BPV cells depends on both intensity and emission spectrum profile of the light source.²⁷ In our experiment, a white LED (emission spectrum in Figure S1) was chosen since its emission fits with the absorption of the microalgae photosynthetic pigments. By tuning the distance

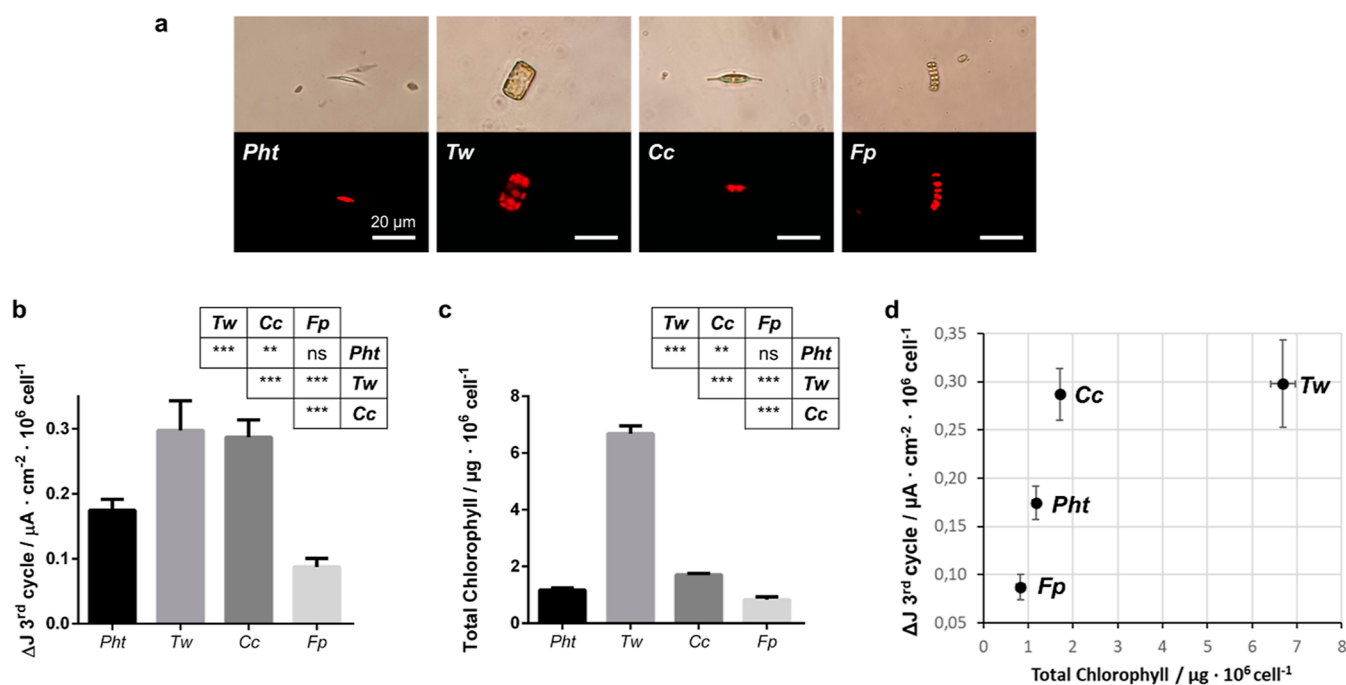


Figure 4. (a) Bright field images of the studied diatom species at 100 \times on top and chloroplast fluorescence images at the bottom. The number of chloroplasts per cell is visible for every single cell (except for Fp, which appears as a chain-like colony of single cells). Scale bar corresponds to 20 μm . (b) Average photocurrent density at the third light cycle from the different species studied, normalized to the number of cells on the bioanode. (c) Total chlorophyll content of each species. Tables report the pairwise tests showing the statistical differences in the chlorophyll content and photocurrent output for the investigated species. (d) Photocurrent values of different species of diatoms on the third cycle of illumination and under the set conditions plotted versus the average total chlorophyll content of each species, normalized to 10^6 cells.

between the BPV cell and the LED, five different irradiance values (10, 30, 54, 100, and 140 $\text{mW} \cdot \text{cm}^{-2}$) were set according to the values commonly used for BPVs' characterization.³⁴ The photocurrent output upon illumination at different light intensities is shown in Figure 3b. A rough increasing linear trend can be observed until 54 $\text{mW} \cdot \text{cm}^{-2}$, reaching a plateau at higher light intensity. This result demonstrates that photocurrent generation by Pht diatoms can be enhanced by increasing light intensity without perturbing the living cells until fairly high intensities of light.

The fabrication of an artificial film of diatoms enables us to study the effect of cell density of the deposited Pht cells on the photocurrent output. When increasing cell density on the WE surface, a significant increase of photocurrent can be observed, until seemingly reaching a plateau at a cell density roughly 10 times larger than the initial one (Figure 3c). However, doubling the cell density does not lead to a doubled value of photocurrent; this suggests that cells closer to the surface of the electrode may transfer electrons more efficiently via the soluble mediator than cells located in more external layers of the film.

Figure 3d shows the photocurrent trend versus the concentration of the K-ferricyanide mediator. A roughly linear trend is observed up to 250 μM concentration, likely due to the fact that below this concentration electrons uptaken from the photosynthetic pathway can efficiently reduce the mediator to K-ferrocyanide that eventually is oxidized at the bioanode.

After the 250 μM concentration threshold, the electron-transfer step from the reduced redox cofactors in the biocatalyst to the artificial redox mediator becomes rate limiting, resulting in the plateau of the obtained photocurrent. In general, this limiting current might vary depending on the properties of the redox mediator utilized and the redox

processes at play, as reported in a work where the rate-determining step in the photocurrent generation from purple bacteria with different diffusible redox mediators was studied.⁴⁰

The K-ferricyanide concentration of 250 μM is sensibly lower than that (1 mM) reported in the literature for a similar setup based on the same microalgal species in suspension.¹⁰ This is a relevant advantage since exogenous mediators such as K-ferricyanide compromise cells' viability if used at a high concentration.⁴¹

Photocurrent Generation Efficiency of Different Diatom Species. After setting the conditions to obtain bioanodes coated with the model Pht cells and to use them as WEs in BPV cells, a comparative study was carried out to evaluate photocurrent generation efficiencies of different diatom species that share common features suitable for their processability onto bioanodes but differ in lifestyle (benthonic, planktonic, or mixed), size, pigment content, and frustule shape. Photocurrent output is expected to depend to some extent on specific cell features. For this aim, three further diatom species were selected as counterparts to the model Pht: the benthonic pinnate diatoms (i) *F. pelliculosa* (Fp) and (ii) *C. closterium* (Cc) and the planktonic, centric (iii) *T. weissflogii* (Tw) with sizes smaller, slightly larger, and much larger than Pht, respectively. Pinnate Fp and Cc were investigated versus pinnate Pht to evaluate possible effects of different sizes, number of chloroplasts per cell, and chlorophyll overall content on photocurrent. Moreover, the centric Tw was studied to compare its photoelectrochemical response with that of pinnate species. Tw is much larger than the other selected diatoms, showing a higher chlorophyll content due to its higher number of chloroplasts (~ 8 –12 for the Tw cell vs 1 for Fp or Pht and 2 for Cc).

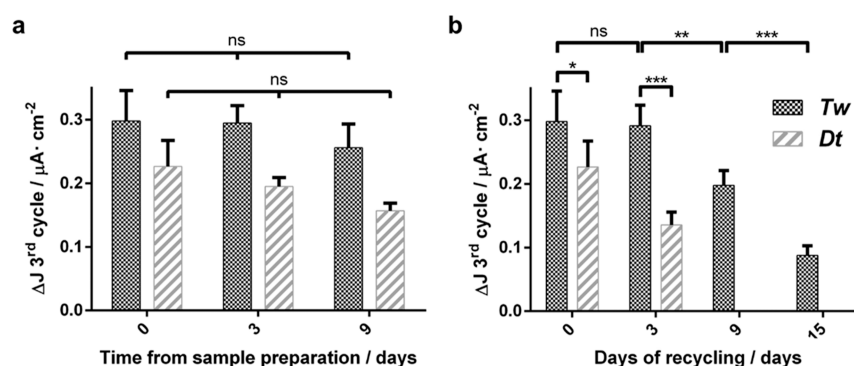


Figure 5. Photocurrent values on the third cycle of illumination under the set conditions for (a) Tw and Dt biophotoanodes after a different number of storage days in dry state. (b) Tw diatoms and green Dt-based biophotoanodes reused for photocurrent extraction four times over a period of 15 days.

Bright field and fluorescence images ($\lambda_{ex} = 488 \text{ nm}$, $\lambda_{em} = 511 \text{ nm}$) were acquired to observe both single diatom cells (Figure 4a) and their films onto electrodes (Figure S3), to evaluate their morphological features and viability. Individual cells and the typical red fluorescence of chlorophyll were observed in all cases. A fixed concentration of $500 \mu M$ K-ferricyanide, higher than the first plateau value of $250 \mu M$ found for Pht, was chosen for the following experiments to avoid any potential side reaction and redox mediator-related photocurrent limitation that may arise from the different microalgal species' capability to reduce K-ferricyanide in solution. Figure 4b,c shows the photocurrent density output recorded at the third illumination cycle for the four different diatoms species and the total chlorophyll amount (expressed as μg per 10^6 cells), respectively. Increasing the size of pinnate species ($Fp < Pht < Cc$), a clear increase of photocurrent density (Figure 4b) and the total chlorophyll amount (Figure 4c) can be observed, and a linear trend of the photocurrent density versus the total chlorophyll amount is evidenced in Figure 4d (dotted line). Conversely, Tw bears an expected higher content of chlorophyll and yet a photocurrent density comparable to that of Cc. Such an effect may be related to a larger surface-to-volume ratio in the case of Tw, in which chloroplasts can be located far from the external cell membrane, limiting their contribution to the photocurrent generation. Such differences may also arise from other key parameters like the species-specific content of enzymes and cofactors involved in intracellular electron transport or in the interaction with the mediator. Hence, the intracellular location, chlorophyll content, and number of chloroplasts may play a relevant role on the ability of diatoms to generate photocurrent, with pinnate diatoms bearing more dense regions of chloroplasts next to the external membrane performing similarly to larger centric diatoms.

The integrity of the films obtained from different species was evaluated by counting the number of cells detached from the film into the solution after a 45 min CA measurement. The average number of detached cells was lower than 2.5% for all species except for Fp (lower than 5.0%, Figure S2), this meaning that detachment does not significantly affect the differences in maximum photocurrent output between species. Therefore, Tw and Cc large species significantly overperform the photocurrent generation of both smaller Pht and Fp.

Tw Displays a Higher Resistance to Repeated Photocurrent Extraction than a Model Green Microalga. Photocurrent generation efficiency of a diatom species

was also compared to that of the model green microalgal species *D. tertiolecta* (Dt) already reported in the literature to produce biophotoanodes in BPVs.^{42,43} Dt was also selected as a marine microalga with well-known endurance to drying and halotolerance.⁴⁴ Tw has several similarities with Dt in terms of cell size (Figure S4a) and marine planktonic behavior. Using the same conditions as for diatoms (see Materials and Methods), a photocurrent density of $0.22 \pm 0.04 \mu A \cdot cm^{-2}$ was detected for Dt-coated biophotoanodes in BPVs (Figure S4, left), this being slightly lower than the values recorded for Cc and Tw and higher than Pht and Fp counterparts (Figure 4b). Moreover, Dt showed an overall chlorophyll content of $\sim 3 \mu g \times 10^{-6} \text{ cells}^{-1}$ (Figure S4b, right), being higher than Pht, Fp, and Cc content and lower than the value recorded for Tw (Figure 4c).

Two different comparative investigations were carried out for Tw- and Dt-coated biophotoanodes. In the first experiment, three sets of bioanodes were fabricated for both Tw and Dt cells (9 electrodes per each species to ensure the analysis in triplicate). Each set was stored in a dry state at RT and indoor ambient light. Photocurrent output of the first set was evaluated immediately after its fabrication, while the second and the third sets of dried electrodes were tested 3 and 9 days after their fabrication, respectively, to evaluate how long-term storage of microalgae kept under dryness can influence their photocurrent generation efficiency over time.

Figure 5a shows that photocurrent values of both species remained almost unchanged over the period of time studied, with the differences in their output being not statistically significant. Therefore, this first experiment did not evidence a significant difference in performance of the Tw diatom versus the Dt green microalga.

As a further comparative investigation, a second experiment was carried out measuring photocurrent densities from two sets (3 electrodes per set for triplicate analysis) of Tw- and Dt-coated biophotoanodes subjected to a drying/wetting cycle between every CA consecutive measurement. In this case, each electrode was used for CA measurements over 15 days. CA was carried out immediately after the drying step needed for the electrode preparation (time = 0). Then, the electrode was dried and stored at RT for 3 days, after which the electrode was rewetted by immersion into the BPV cell for the second CA. Redrying and dry storage was repeated twice for a further 6 days, thus performing further CAs at the ninth and 15th days from the electrode fabrication, to evaluate the photocurrent

output and resistance of cells versus prolonged storage time and reuse in a BPV device.

On day 0, the average Tw and Dt photocurrents were similar to those recorded in the first experiment. On day 3, the photocurrent recorded for Tw remained unchanged ($98 \pm 5\%$), while the Dt photocurrent significantly decreased to $60 \pm 3\%$ versus the value at time 0 (Figure 5b). After 9 to 15 days, the Tw photocurrent gradually decreased to $66 \pm 7\%$ and $30 \pm 3\%$, respectively. Conversely, the Dt photocurrent dropped to an undetectable value already at the ninth day. Comparison of FDA assays for Tw and Dt cells at day 0 and day 15 after four CAs in Figure S5a confirms that Tw cells are more viable than Dt cells ($\sim 23\%$ vs $\sim 6\%$). It is worth noting that, despite observing a weak fluorescence for Dt cells, their photocurrents are negligible, indicating a possible compromised capability of the survived Dt cells to reduce K-ferricyanide. Figure S5b,c also shows that the reduced Dt photocurrents are not due to a higher proportion of fallen cells after 15 days because the deposited cells still persist onto the electrode.

This comparative result with respect to a well-known green microalgal species *D. tertiolecta* strengthens the evidence that diatom microalgae, such as *T. weissflogii*, are very promising candidates for biophotovoltaic applications.²⁸

Higher resistance to drying/wetting cycles of diatoms versus green microalgae might be related to diatom peculiar mesoporous biosilica shells that protect their organic protoplasm from external noxious factors and stress, such as exogenous viruses or aggressive chemicals, persistent or intense UV-blue light irradiation, and limited water availability. Further aspects that might differently affect the photocurrent response of the two microalgal species over time are the application of an external potential and the presence of an exogenous soluble mediator in the BPV cell. However, these hypotheses require further investigation to shed light on the effective factors responsible for the higher resistance to dryness of Tw diatoms versus the green Dt cells.

Internal Quantum Efficiency of BPVs. The IQE, defined as the ratio between the number of electrons pumped into the circuit and the number of photons transferred to the anode,⁴⁵ is a common figure of merit for BPVs. For IQE calculation (eqs 1–4 in S6), a monochromatic lighting source was required to evaluate the number of photons that radiate cells.⁴² For this aim, a red LED emitting at 660 nm with a full width at half-maximum of 40 nm was used (Figure S1). IQE values of $0.072 \pm 0.015\%$ and $0.026 \pm 0.007\%$ were obtained under the standard conditions for Tw and Dt, respectively. This result is another proof that Tw overperforms Dt in a BPV. Moreover, the IQE for Tw is similar to that reported in the literature for optimized BPV devices based on cyanobacteria,⁴² and considering that our BPV setup was selected to be as simple as possible, such a similarity highlights the effective suitability of diatoms as candidates of election for the fabrication of efficient BPVs.

CONCLUSION

In summary, diatoms are valuable candidates for the fabrication of biophotoanodes in BPVs, with photocurrent generation efficiencies depending on the microalgal species used to coat the electrode, as well as on the intensity of the lighting source and on the cell density at the bioanode surface. A linear trend of photocurrent is observed with increasing light intensity, showing that the highest irradiance used ($140 \text{ mW}\cdot\text{cm}^{-2}$) triggers a photoresponse while not altering living cells. A

linear increase of photocurrent is also observed when increasing cell density on the WE surface, with photocurrent values likely being more dependent on the number of cells in close contact with the electrode. A further advantage observed for biophotoanodes based on diatoms is that BPVs require lower amount of mediator with respect to already reported bioanodes working with different photosynthetic microorganisms such as bacteria.⁴¹

Our study also evidences that the photocurrent output of BPVs based on different diatom species varies depending on the total chlorophyll content per cell, with the best results recorded for *T. weissflogii* and *C. closterium* with respect to *P. tricornutum* and *F. pelliculosa* species.

Moreover, for the first time, we have demonstrated a valuable resistance to dryness of biophotoanodes made with *T. weissflogii* diatoms versus *D. tertiolecta* green microalgae, paving the way for the fabrication of highly robust diatom-based biophotovoltaic devices whose electrodes can be stored for a long time under water starvation without altering their efficiency after wetting. This finding is of critical relevance, since desiccation resistance and prolonged use are valued properties of stable living biophotoanodes, for applications ranging from photocurrent production to biosensing.

Future work will be focused on optimization of the simple BPV configuration studied herein. Possible strategies to optimize device performances include the use of highly nanoporous electrodes to increase their available electroactive surface, the incorporation of diatoms in redox polymers, the selection of the best redox mediators, or even the development of methods avoiding mediators, as well as the use of cell culture medium as the electrolyte to promote diatom growth directly inside BPVs.

ASSOCIATED CONTENT

Supporting Information

The Supporting Information is available free of charge at <https://pubs.acs.org/doi/10.1021/acssuschemeng.4c00935>.

Light emission spectra from different light sources used; average number of fallen cells from bioanodes after CA; morphological analysis of biophotoanodes; morphological information, photocurrent, and chlorophyll content from *D. tertiolecta*; and equations needed to calculate the IQE (PDF)

AUTHOR INFORMATION

Corresponding Authors

Roberta Ragni – Dipartimento di Chimica, Università Degli Studi di Bari “Aldo Moro”, Bari I-70126, Italy; orcid.org/0000-0002-0451-7096; Email: roberta.ragni@uniba.it

Gianluca M. Farinola – Dipartimento di Chimica, Università Degli Studi di Bari “Aldo Moro”, Bari I-70126, Italy; orcid.org/0000-0002-1601-2810; Email: gianlucamaria.farinola@uniba.it

Authors

Cesar Vicente-Garcia – Dipartimento di Chimica, Università Degli Studi di Bari “Aldo Moro”, Bari I-70126, Italy; orcid.org/0000-0002-0438-4887

Daniilo Vona – Dipartimento di Scienze Del Suolo, Della Pianta e Degli Alimenti, Università Degli Studi di Bari “Aldo Moro”, Bari I-70126, Italy

Francesco Milano – Istituto di Scienze Delle Produzioni Alimentari, Consiglio Nazionale Delle Ricerche, Lecce I-73100, Italy; orcid.org/0000-0001-5453-2051

Gabriella Buscemi – Dipartimento di Chimica, Università Degli Studi di Bari “Aldo Moro”, Bari I-70126, Italy

Matteo Grattieri – Dipartimento di Chimica, Università Degli Studi di Bari “Aldo Moro”, Bari I-70126, Italy; orcid.org/0000-0002-1795-3655

Complete contact information is available at:

<https://pubs.acs.org/10.1021/acssuschemeng.4c00935>

Author Contributions

The manuscript was written through contributions of all authors. All authors have given approval to the final version of the manuscript.

Funding

This work was supported by H2020-MSCA-ITN-2019 project 860125-BEEP (Bioinspired and bionic materials for enhanced photosynthesis).

Notes

The authors declare no competing financial interest.

ACKNOWLEDGMENTS

The authors thank Prof. Bruno Freire Boa de Jesus from the Nantes Université for generously supplying the *C. closterium* diatom strain; Dr. Giusy D’Attoma for her help in the viability assay; and Dr. Gabriella Leone for preliminary experiments on diatom cultures.

ABBREVIATIONS

BPV, biophotovoltaic; Pht, *Phaeodactylum tricornutum*; Tw, *Thalassiosira weissflogii*; Fp, *Fistulifera pelliculosa*; Cc, *Cylindrotheca closterium*; Dt, *Dunaliella tertiolecta*; MFC, microbial fuel cell; BPEC, biophotoelectrochemical cell; FR, ferriredutase; ITO, indium tin oxide; FDA, fluorescein diacetate; PAR, photosynthetically active radiation; RT, room temperature; PB, phosphate buffer; IQE, internal quantum efficiency; CA, chronoamperometry; DMF, dimethylformamide

REFERENCES

- (1) Hughes, S. R.; Jones, M. A. *The Global Demand for Biofuels and Biotechnology-Derived Commodity Chemicals*; Technologies, Markets, and Challenges, 2020.
- (2) Moriarty, P.; Honnery, D. Review: Renewable Energy in an Increasingly Uncertain Future. *Appl. Sci.* **2023**, *13* (1), 388.
- (3) Gallagher, J.; Basu, B.; Browne, M.; Kenna, A.; McCormack, S.; Pilla, F.; Styles, D. Adapting Stand-Alone Renewable Energy Technologies for the Circular Economy through Eco-Design and Recycling. *J. Ind. Ecol.* **2019**, *23* (1), 133–140.
- (4) Santoro, C.; Arbizzani, C.; Erable, B.; Ieropoulos, I. Microbial Fuel Cells: From Fundamentals to Applications. A Review. *J. Power Sources* **2017**, *356*, 225–244.
- (5) Beaver, K.; Gaffney, E. M.; Minter, S. D. Understanding Metabolic Bioelectrocatalysis of the Purple Bacterium *Rhodobacter Capsulatus* through Substrate Modulation. *Electrochim. Acta* **2022**, *416* (February), 140291.
- (6) Shlosberg, Y.; Schuster, G.; Adir, N. Harnessing Photosynthesis to Produce Electricity Using Cyanobacteria, Green Algae, Seaweeds and Plants. *Front. Plant Sci.* **2022**, *13* (July), 1–15.
- (7) Bombelli, P.; Savanth, A.; Scarampi, A.; Rowden, S. J. L.; Green, D. H.; Erbe, A.; Årsløt, E.; Jevremovic, I.; Hohmann-Marriott, M. F.; Trasatti, S. P.; et al. Powering a Microprocessor by Photosynthesis. *Energy Environ. Sci.* **2022**, *15* (6), 2529–2536.

- (8) Roxby, D. N.; Yuan, Z.; Krishnamoorthy, S.; Wu, P.; Tu, W. C.; Chang, G. E.; Lau, R.; Chen, Y. C. Enhanced Biophotocurrent Generation in Living Photosynthetic Optical Resonator. *Adv. Sci.* **2020**, *7* (11), 1903707.
- (9) Shlosberg, Y.; Krupnik, N.; Tóth, T. N.; Eichenbaum, B.; Meirovich, M. M.; Meiri, D.; Yehezkeili, O.; Schuster, G.; Israel, A.; Adir, N. Bioelectricity Generation from Live Marine Photosynthetic Macroalgae: Bioelectricity from Macroalgae. *Biosens. Bioelectron.* **2022**, *198* (November 2021), 113824.
- (10) Laohavisit, A.; Anderson, A.; Bombelli, P.; Jacobs, M.; Howe, C. J.; Davies, J. M.; Smith, A. G. Enhancing Plasma Membrane NADPH Oxidase Activity Increases Current Output by Diatoms in Biophotovoltaic Devices. *Algal Res.* **2015**, *12*, 91–98.
- (11) Khan, M. J.; Das, S.; Vinayak, V.; Pant, D.; Ghangrekar, M. M. Live Diatoms as Potential Biocatalyst in a Microbial Fuel Cell for Harvesting Continuous Diafuel, Carotenoids and Bioelectricity. *Chemosphere* **2022**, *291* (P1), 132841.
- (12) Malviya, S.; Scalco, E.; Audic, S.; Vincent, F.; Veluchamy, A.; Poulain, J.; Wincker, P.; Iudicone, D.; De Vargas, C.; Bittner, L.; et al. Insights into Global Diatom Distribution and Diversity in the World’s Ocean. *Proc. Natl. Acad. Sci. U.S.A.* **2016**, *113* (11), E1516–E1525.
- (13) Leterme, S. C.; Prime, E.; Mitchell, J.; Brown, M. H.; Ellis, A. V. Diatom Adaptability to Environmental Change: A Case Study of Two *Cocconeis* Species from High-Salinity Areas. *Diatom Res.* **2013**, *28* (1), 29–35.
- (14) Zhao, P.; Gu, W.; Wu, S.; Huang, A.; He, L.; Xie, X.; Gao, S.; Zhang, B.; Niu, J.; Peng Lin, A.; et al. Silicon Enhances the Growth of *Phaeodactylum tricornutum* Bohlin under Green Light and Low Temperature. *Sci. Rep.* **2014**, *4*, 3958.
- (15) Dhaouadi, F.; Awwad, F.; Diamond, A.; Desgagné-Penix, I. Diatoms’ Breakthroughs in Biotechnology: *Phaeodactylum tricornutum* as a Model for Producing High-Added Value Molecules. *Am. J. Plant Sci.* **2020**, *11* (10), 1632–1670.
- (16) Vinayak, V.; Khan, M. J.; Varjani, S.; Saratale, G. D.; Saratale, R. G.; Bhatia, S. K. Microbial Fuel Cells for Remediation of Environmental Pollutants and Value Addition: Special Focus on Coupling Diatom Microbial Fuel Cells with Photocatalytic and Photoelectric Fuel Cells. *J. Biotechnol.* **2021**, *338* (July), 5–19.
- (17) Cicco, S. R.; Vona, D.; Leone, G.; De Giglio, E.; Bonifacio, M. A.; Cometa, S.; Fiore, S.; Palumbo, F.; Ragni, R.; Farinola, G. M. In Vivo Functionalization of Diatom Biosilica with Sodium Alendronate as Osteoactive Material. *Mater. Sci. Eng., C* **2019**, *104* (June), 109897.
- (18) Ragni, R.; Cicco, S. R.; Vona, D.; Farinola, G. M. Multiple Routes to Smart Nanostructured Materials from Diatom Microalgae: A Chemical Perspective. *Adv. Mater.* **2018**, *30* (19), No. e1704289.
- (19) Jeffries, C.; Campbell, J.; Li, H.; Jiao, J.; Rorrer, G. The Potential of Diatom Nanobiotechnology for Applications in Solar Cells, Batteries, and Electroluminescent Devices. *Energy Environ. Sci.* **2011**, *4* (10), 3930–3941.
- (20) Vona, D.; Cicco, S. R.; Labarile, R.; Flemma, A.; Garcia, C. V.; Giangregorio, M. M.; Cotugno, P.; Ragni, R. Boronic Acid Moieties Stabilize Adhesion of Microalgal Biofilms on Glassy Substrates: A Chemical Tool for Environmental Applications. *ChemBioChem* **2023**, *24*, No. e202300284.
- (21) Tong, C. Y.; Derek, C. J. C. Biofilm Formation of Benthic Diatoms on Commercial Polyvinylidene Fluoride Membrane. *Algal Res.* **2021**, *55* (February), 102260.
- (22) Gügi, B.; Le Costaouec, T.; Burel, C.; Lerouge, P.; Helbert, W.; Bardor, M. Diatom-Specific Oligosaccharide and Polysaccharide Structures Help to Unravel Biosynthetic Capabilities in Diatoms. *Mar. Drugs* **2015**, *13* (9), 5993–6018.
- (23) Ciglenečki, I.; Dautović, J.; Cvitešić, A.; Pletikapić, G. Production of Surface Active Organic Material and Reduced Sulfur Species during the Growth of Marine Diatom *Cylindrotheca closterium*. *Croat. Chem. Acta* **2018**, *91* (4), 455–461.
- (24) Torquato, L. D. d. M.; Grattieri, M. Photobioelectrochemistry of Intact Photosynthetic Bacteria: Advances and Future Outlook. *Curr. Opin. Electrochem.* **2022**, *34*, 101018.

- (25) Gupta, S.; Agrawal, S. C. Survival and Motility of Diatoms Navicula Grimmei and Nitzschia Palea Affected by Some Physical and Chemical Factors. *Folia Microbiol.* **2007**, *52* (2), 127–134.
- (26) Souffreau, C.; Vanormelingen, P.; Verleyen, E.; Sabbe, K.; Vyverman, W. Tolerance of Benthic Diatoms from Temperate Aquatic and Terrestrial Habitats to Experimental Desiccation and Temperature Stress. *Phycologia* **2010**, *49* (4), 309–324.
- (27) Sawa, M.; Fantuzzi, A.; Bombelli, P.; Howe, C. J.; Hellgardt, K.; Nixon, P. J. Electricity Generation from Digitally Printed Cyanobacteria. *Nat. Commun.* **2017**, *8* (1), 1327.
- (28) Gacitua, M.; Urrejola, C.; Carrasco, J.; Vicuña, R.; Sraín, B. M.; Pantoja-Gutiérrez, S.; Leech, D.; Antiochia, R.; Tasca, F. Use of a Thermophile Desiccation-Tolerant Cyanobacterial Culture and Os Redox Polymer for the Preparation of Photocurrent Producing Anodes. *Front. Bioeng. Biotechnol.* **2020**, *8* (August), 900.
- (29) Kustka, A. B.; Shaked, Y.; Milligan, A. J.; King, D. W.; Morel, F. M. M. Extracellular Production of Superoxide by Marine Diatoms: Contrasting Effects on Iron Redox Chemistry and Bioavailability. *Limnol. Oceanogr.* **2005**, *50* (4), 1172–1180.
- (30) Carmel, N.; Tel-Or, E.; Chen, Y.; Pick, U. Iron Uptake Mechanism in the Chrysophyte Microalga Dinobryon. *J. Plant Physiol.* **2014**, *171* (12), 993–997.
- (31) Anderson, A.; Laohavisit, A.; Blaby, I. K.; Bombelli, P.; Howe, C. J.; Merchant, S. S.; Davies, J. M.; Smith, A. G. Exploiting Algal NADPH Oxidase for Biophotovoltaic Energy. *Plant Biotechnol. J.* **2016**, *14* (1), 22–28.
- (32) Buscemi, G.; Vona, D.; Stufano, P.; Labarile, R.; Cosma, P.; Agostiano, A.; Trotta, M.; Farinola, G. M.; Grattieri, M. Bio-Inspired Redox-Adhesive Polydopamine Matrix for Intact Bacteria Biohybrid Photoanodes. *ACS Appl. Mater. Interfaces* **2022**, *14* (23), 26631–26641.
- (33) Garvey, M.; Moriceau, B.; Passow, U. Applicability of the FDA Assay to Determine the Viability of Marine Phytoplankton under Different Environmental Conditions. *Mar. Ecol.: Prog. Ser.* **2007**, *352*, 17–26.
- (34) Wey, L. T.; Bombelli, P.; Chen, X.; Lawrence, J. M.; Rabideau, C. M.; Rowden, S. J. L.; Zhang, J. Z.; Howe, C. J. The Development of Biophotovoltaic Systems for Power Generation and Biological Analysis. *ChemElectroChem* **2019**, *6* (21), 5375–5386.
- (35) Vona, D.; Ragni, R.; Altamura, E.; Albanese, P.; Giangregorio, M. M.; Cicco, S. R.; Farinola, G. M. Light-emitting Biosilica by in Vivo Functionalization of Phaeodactylum Tricornutum Diatom Microalgae with Organometallic Complexes. *Appl. Sci.* **2021**, *11* (8), 3327.
- (36) Ng, F. L.; Phang, S. M.; Periasamy, V.; Yunus, K.; Fisher, A. C. Evaluation of Algal Biofilms on Indium Tin Oxide (ITO) for Use in Biophotovoltaic Platforms Based on Photosynthetic Performance. *PLoS One* **2014**, *9* (5), No. e97643.
- (37) Tucci, M.; Bombelli, P.; Howe, C. J.; Vignolini, S.; Bocchi, S.; Schievano, A. A Storable Mediatorless Electrochemical Biosensor for Herbicide Detection. *Microorganisms* **2019**, *7* (12), 630.
- (38) Elisabeth, B.; Rayen, F.; Behnam, T. Microalgae Culture Quality Indicators: A Review. *Crit. Rev. Biotechnol.* **2021**, *41* (4), 457–473.
- (39) Rico, M.; López, A.; Santana-Casiano, J. M.; González, A. G.; González-Dávila, M. Variability of the Phenolic Profile in the Diatom Phaeodactylum Tricornutum Growing under Copper and Iron Stress. *Limnol. Oceanogr.* **2013**, *58* (1), 144–152.
- (40) Grattieri, M.; Rhodes, Z.; Hickey, D. P.; Beaver, K.; Minter, S. D. Understanding Biophotocurrent Generation in Photosynthetic Purple Bacteria. *ACS Catal.* **2019**, *9* (2), 867–873.
- (41) Sayegh, A.; Perego, L. A.; Arderiu Romero, M.; Escudero, L.; Delacotte, J.; Guille-Collignon, M.; Grimaud, L.; Bailleul, B.; Lemaître, F. Finding Adapted Quinones for Harvesting Electrons from Photosynthetic Algae Suspensions. *ChemElectroChem* **2021**, *8* (15), 2968–2978.
- (42) McCormick, A. J.; Bombelli, P.; Scott, A. M.; Philips, A. J.; Smith, A. G.; Fisher, A. C.; Howe, C. J. Photosynthetic Biofilms in Pure Culture Harness Solar Energy in a Mediatorless Bio-Photovoltaic Cell (BPV) System. *Energy Environ. Sci.* **2011**, *4* (11), 4699–4709.
- (43) Shlosberg, Y.; Tóth, T. N.; Eichenbaum, B.; Keysar, L.; Schuster, G.; Adir, N. Electron Mediation and Photocurrent Enhancement in Dunaliella Salina Driven Bio-Photo Electrochemical Cells. *Catalysts* **2021**, *11* (10), 1220.
- (44) Liang, M. H.; Qy, X. Y.; Chen, H.; Wang, Q.; Jiang, J. G. Effects of Salt Concentrations and Nitrogen and Phosphorus Starvations on Neutral Lipid Contents in the Green Microalga Dunaliella Tertiolecta. *J. Agric. Food Chem.* **2017**, *65* (15), 3190–3197.
- (45) Lo Presti, M.; Giangregorio, M. M.; Ragni, R.; Giotta, L.; Guascito, M. R.; Comparelli, R.; Fanizza, E.; Tangorra, R. R.; Agostiano, A.; Losurdo, M.; et al. Photoelectrodes with Polydopamine Thin Films Incorporating a Bacterial Photoenzyme. *Adv. Electron. Mater.* **2020**, *6* (7), 2000140.